

VYSOKÉ UČENÍ TECHNICKÉ V BRNĚ
BRNO UNIVERSITY OF TECHNOLOGY

FAKULTA STROJNÍHO INŽENÝRSTVÍ
FACULTY OF MECHANICAL ENGINEERING

ÚSTAV MATEMATIKY
INSTITUTE OF MATHEMATICS

ING. RŮŽENA JANOUTOVÁ

MODELLING 3D FOREST STRUCTURE
FOR IMPROVED RETRIEVAL OF FOREST
BIOPHYSICAL PROPERTIES

MODELOVÁNÍ 3D STRUKTURY LESA PRO ZLEPŠENÍ
ODHADŮ BIOFYZIKÁLNÍCH VLASTNOSTÍ LESA

zkrácená verze dizertační práce

Studijní obor: Aplikovaná matematika

Vedoucí práce: doc. PaedDr. Dalibor Martišek, Ph.D.

Keywords

radiative transfer model, DART, 3D spruce model, estimation of vegetation parameters

Klíčová slova

model přenosu záření, DART, 3D model smrku, odhady vegetačních parametrů

The Ph.D. Thesis is available in the library of the Faculty of Mechanical Engineering, Brno University of Technology.

Table of contents

1	Introduction	2
1.1	Thesis structure and synopsis	2
1.2	Research goals	3
2	Theoretical background	5
2.1	3D spruce model	5
2.2	Radiative transfer modeling	5
2.2.1	PROSPECT	6
2.2.2	DART	6
2.3	Estimation of vegetation parameters from remote sensing data	6
3	Experimental part	7
3.1	Study sites	7
3.2	Input data	7
3.2.1	Distribution of shoots and measurements of tree skeleton structure	7
3.2.2	Field measurements of biochemical and biophysical properties	7
3.2.3	Remote Sensing data	7
3.3	Reconstruction of virtual Norway spruce 3D tree models	7
3.3.1	Reconstruction of wooden skeletons - trunks and main branches	9
3.3.2	Translation and scaling of the foliage point cloud	9
3.3.3	Algorithm for shoot distribution within spruce crown	10
3.3.4	Main outcome	12
3.4	Radiative transfer modeling and optimization	16
3.4.1	DART scenes	16
3.4.2	Optimization at shoot level	17
3.4.3	Optimization at tree level	18
3.4.4	Optimization at canopy level	18
3.4.5	Main outcome	19
3.5	Estimation of quantitative vegetation parameters	20
3.5.1	LUT creation	21
3.5.2	Estimation of Cab and LAI	22
3.5.3	Validation against the field data	25
3.5.4	Main outcome	26
4	Synthesis and outlook	27
4.1	Main conclusions and impact	27
4.2	Potential improvements	27
4.3	Possible application of the 3D spruce model	27
	References	29
	Curriculum vitae	32

1 | Introduction

1.1 Thesis structure and synopsis

Remote sensing (RS) is a multidisciplinary scientific domain for measuring the electromagnetic radiance reflected and radiated from Earth surfaces. One kind of RS imaging spectroscopy data is called hyperspectral spectroscopy. It contains tens to hundreds reflectance images representing very narrow wavelength intervals within the continuous optical spectral range of 400 – 2500 nm. The hyperspectral images are frequently used for mapping of vegetation traits such as content of chlorophylls a+b (Cab), leaf area index (LAI), etc.

Methods of quantitative estimation of plant Cab using proximal and RS data can be divided in two major groups: i) empirical and ii) physical approaches (Liang 2005). Empirical approaches build on a simple regression relationship established between field measured Cab and reflectance data (Curran et al. 2001; Gitelson et al. 2003; Main et al. 2011). Physical approaches use radiative transfer models (RTM), for instance the Discrete Anisotropic Radiative Transfer (DART) model (Gastellu-Etchegorry et al. 2015), to simulate plant-light interactions. RTMs provide an explicit link between their outputs, simulated top-of-canopy reflectance, and input characteristics, i.e. biochemical and structural properties of the main scattering elements – leaves (Jacquemoud et al. 2009).

The thesis is consisting of several consecutive methodological steps illustrated in Figure 1.1: i) creation of representative 3D spruce tree model from terrestrial laser scanning data, ii) three-level optimization of the 3D tree model, iii) DART forward simulations of spruce forest, and iv) estimation and validation of Cab and LAI from the Sentinel-2 satellite image.

The wooden skeleton of a tree is an important part of the 3D spruce model. It contributes to reflected radiance of a whole forest stand scene due to a high near infrared reflectance, especially in cases of low LAI and sparse forest canopy cover. The reconstruction of wooden skeleton was realized with an automatic algorithm designed by Sloup (2013), which uses the terrestrial Light Detection and Ranging (LiDAR) scans of single trees. The LiDAR point cloud are also used for virtual distribution of needle-age classes shoots within a tree crown.

Correct shoot distribution and assignment of the foliage optical properties within a spruce tree crown is not an easy task. The Norway spruce is an evergreen tree, which means that its crown contains shoots of several (on average five) ages. Needles of current year have significantly different optical properties when compared to older needles, whereas the differences among older age classes are much less significant. It is important to characterize these differences in our model, because they play an important role in estimation of quantitative parameters of whole canopy. Unfortunately, the shoot age is not the only aspect influencing optical properties of needles. Another important aspect is the amount and canopy penetration of incoming photosynthetically active solar irradiance, which stimulates growth of new foliage and consequently the number of current year needles in vertical profile of tree crown. Therefore, a new algorithm had to be designed for correct distribution of needle shoots in spruce crown, which is one of the main outcomes of this thesis.

It must be acknowledged that the reflectance of forests, captured in remotely sensed data, is strongly modulated by its architecture and canopy structure. Different approaches allow one to consider the architectural and structural forest features when simulating remote sensing optical data in RTMs. The traditional approach in the DART model, considered in this study as the base model, is to treat forest as a 3D matrix of voxels (cells) shaped

geometrically in crowns and filled with a homogeneous turbid medium of foliage particles. Each vegetation turbid cell contains virtual particles with predefined optical and structural properties of leaves, in our case the shoots of needles. The density and the geometrical distribution of turbid medium particles is determined by the LAI and the leaf angle distribution (LAD) and other vegetation structural parameters of the DART model. However, this approach is not always fully satisfactory, because $\alpha(\Omega)$ is an empirically derived weight and because LAD is defined as a simplified function, which might not be able to properly describe the complex spruce structure. As the result, the direct comparison of DART top-of-canopy reflectance simulations and RS observation shows in some cases significant intensity differences (Figure 3.8a). This discrepancy is the main motivation for improvement of spruce forest simulation in the DART model. One of the key DART inputs are tree representations - 3D models, which characterize architecture of each forest species. Compared to the base turbid-cell models, the explicit 3D tree models are highly computationally demanding, and in case of too large forested scenes with large amount of trees unfeasible to simulate.

Therefore, an optimization of 3D spruce model at three scale levels (shoots, tree crowns, and canopy) was conducted. Two new simplified shoot models were designed and their reflectance simulated with the DART model was cross-compared with reflectance of i) an original geometrically complex shoot containing single needles (reference shoot) and ii) a shoot previously simplified by DART developers. DART simulations with new shoots, implemented in a single-tree mock-up, were compared with the same simulation of exact 3D spruce model, converted and original turbid cell tree, as well as real airborne data. Since it was impossible to use 3D spruce model in whole forest stand simulations, only the last two comparisons were performed at the canopy level.

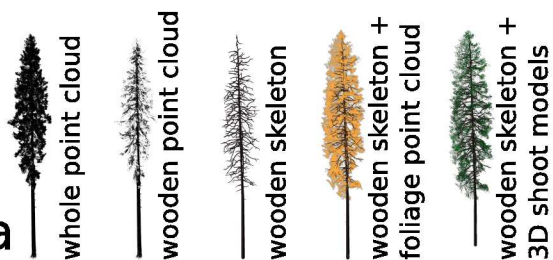
The final part of this study is devoted to estimation of the two vegetation parameters, Cab and LAI, retrieved from satellite RS image using the DART simulations over the optimized representation of the spruce canopy. Accuracy of the estimations is compared with those achieved using the base turbid cell model.

1.2 Research goals

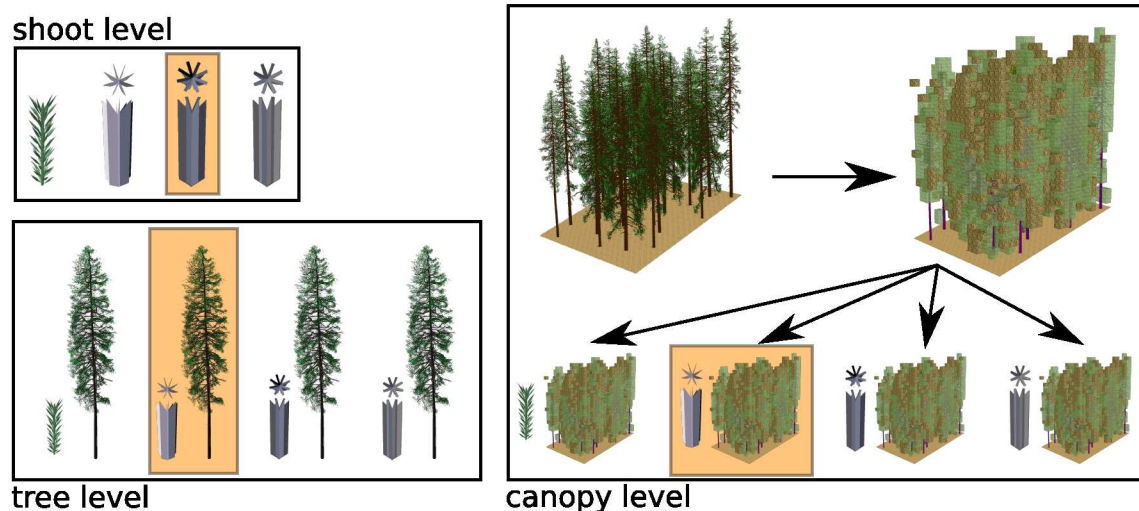
The main goal of this study is to improve accuracy of quantitative vegetation parameters for Norway spruce stand estimated through inversion of the DART model. This main goal can be divided in the following specific aims:

1. Creation of the geometrically precise 3D model of Norway spruce (*Picea abies* [L.] Karst.) according to point clouds obtained for individual trees at the Bílý Kříž study site with the terrestrial laser scanning approach (Section 3.3).
2. Optimization of computationally too demanding 3D spruce model for operational implementation in RTM, specifically in the DART model.
3. Assessment of improvements due to the new 3D spruce model and its derivate, i.e. a converted turbid cell models of spruce trees. This aim can be broken down in three consecutive steps:
 - Creation of an optimized spruce forest stand DART scene and simulation of a DART reflectance look-up-tables (LUT).
 - Retrieval of spruce canopy parameters from a multispectral satellite image through an inversion using DART LUT.
 - Validation and accuracy assessment of the estimates through comparison with field Cab and LAI measurements.

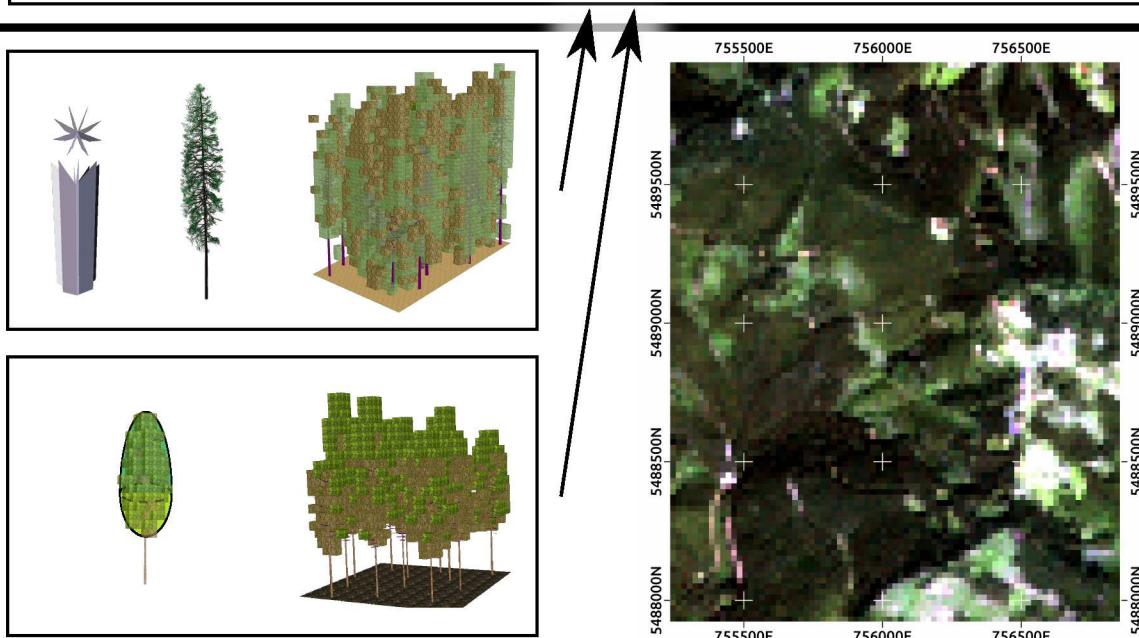
creating of
3D spruce model
from laser scanning data



3D spruce model optimization at three levels



DART - radiative transfer modelling



estimation of vegetation parameters from remote sensing satellite data and validation

Figure 1.1: The workflow diagram of this thesis. The orange boxes indicate the optimal solution for each optimization level.

2 | Theoretical background

At the beginning, it is needed to define terms used throughout this thesis. The theoretical part is separated into three main sections. First, the theory concerning the creation of the 3D spruce model, second, the theory connected to radiative transfer modelling, and third, the theory behind estimation of vegetation parameters from RS data is described here. Because the topic of this thesis is very wide, it combines different fields of mathematics and physics, therefore not every single term is defined in details. The precise definitions are used only for the terms used directly in this thesis and for instances with multiple definitions.

2.1 3D spruce model

Creation of the 3D spruce model is one of the main goals and it is necessary to define theory behind algorithms designed in this study. The 3D spruce model based on LiDAR data was created, therefore the first part of this section introduces theory of laser scanning (Section 2.1).

Laser scanning

Portable terrestrial laser scanning systems are increasingly being used for studies of canopy structure from the ground. LiDAR systems employ similar principles to radar systems. The laser sends out a series of very short pulses of a very narrow beam of coherent light, in a precise waveband; the time delay of the reflected pulse can then be used to determine the distance between the sensor and the reflecting surface. This section was adapted from Jones & Vaughan (2010).

2.2 Radiative transfer modeling

In remote sensing the usual requirement is to determine the surface reflectance and to make use of this in inferring canopy or surface biophysical characteristics. The use of bidirectional reflectance data greatly enhances the capacity to extract canopy biophysical information when coupled with appropriate radiative transfer (RT) modelling. The various radiative transfer models available vary in the detail in which they treat the anisotropy of the radiation field in canopies. In such modelling it is often convenient to treat the radiation field as the sum of a number of components. These could include the unscattered irradiance, radiation that has been scattered once, and multiply scattered irradiance that has been scattered several times. This paragraph was adapted from Jones & Vaughan (2010).

There are two types of Radiative Transfer Models (RTMs), at the leaf-level and at the canopy-level. Leaf-level models simulate optical properties i.e. light reflectance and transmittance through a leaf. Among the leaf-level RTMs, the PROSPECT model (Jacquemoud & Baret 1990; Feret et al. 2008) is probably the most widely used.

Canopy-level RTM effectively scales the leaf optical properties to the level of plant canopies (e.g. agricultural fields, forests). There has been a large number of canopy RTMs developed and they span from relatively simple ones to complex, computationally demanding 3D models. A good overview of currently used canopy RTMs is provided at the website of Radiation transfer Model Intercomparison (RAMI, <http://rami-benchmark.jrc.ec.europa.eu>).

Canopy RTMs that attempt to reproduce the complex architecture of trees and forests are naturally more suitable to interpret remote sensing (RS) data acquired over forested areas. In this thesis the DART model was used.

2.2.1 PROSPECT

PROSPECT simulates leaf reflectance and transmittance (HTRF) from the visible (VIS) to the middle infrared spectrum as a function of the leaf structure parameter and leaf biochemical parameters (Jacquemoud and Baret 1990). It is based on so-called “plate model” developed by Allen et al. (1969), who represented a leaf as a uniform plate with rough surfaces. The leaf reflectance and transmittance (HTRF) are determined in the plate model using geometric optical principles. The fixed parameters include the index of refraction and absorption coefficients of the main absorbing constituents (C_{ab} , C_{ar} , C_m , and C_w). This section is adapted from Jones & Vaughan (2010).

In this thesis were used two versions of the PROSPECT model 3S and 5. The PROSPECT 3S model was adjusted to recalibrated to Norway spruce needles by Malenovský et al. (2006) and it calculates leaf reflectance and transmittance (HTRF) in the range from 450 to 1000 nm as functions of four input parameters: C_{ab} , C_w , C_m , and N . The PROSPECT 5 model differs in the reflectance range from 400 to 2500 nm and number of input parameters: C_{ab} , C_{ar} , C_m , C_w , N . (Jacquemoud & Baret 1990; Feret et al. 2008).

2.2.2 DART

The DART model simulates the radiative budget and RS data (images of radiometers, LiDAR waveforms, and photon counting) of any Earth scene (natural/urban, with/without relief) for any sun direction, atmosphere and viewing direction in optical and thermal domain (CESBIO 2015, Gastellu-Etchegorry et al. 2015). The DART model is able to simulate detailed complex scenes with 3D objects and is able to simulate RS images, therefore it was chosen for simulating spruce forest scenes for this thesis.

2.3 Estimation of vegetation parameters from remote sensing data

Some quantitative vegetation parameters, which are propagated in optical spectra, could be estimated with several retrieval methods from RS data. The physically based retrieval approaches use inversion of RTM. Commonly employed inversion methods include direct iterative optimization, inversions of look-up-tables (LUT), and machine learning algorithms.

Use of modern machine learning methods for retrieval of vegetation parameters is increasing lately. Machine learning is a prolific field of research, producing algorithms that are able to cope with strong nonlinearity and high dimensionality of the data. They typically use RTM simulated LUTs for training to build a non-parametric statistical inversion model (Schlerf & Atzberger 2006; Verrelst et al. 2012a). Among the most popular machine learning methods are artificial neural networks and support vector machines (SVM). Even more recent methods, such as kernel ridge regression and Gaussian process regression (Verrelst et al., 2012b), showed promising results in terms of performance of retrieval and computing efficiency.

This section was adopted from Homolová et al. (2015b).

3 | Experimental part

3.1 Study sites

The study was conducted in Norway spruce stand at the permanent ecological research site Bílý Kříž (Moravian-Silesian Beskids) and additional datasets were acquired from the Černá hora study site (Šumava National Park). Detailed description of both research sites is provided in the following sections.

3.2 Input data

3.2.1 Distribution of shoots and measurements of tree skeleton structure

Shoot distribution data available in scientific literature (Barták 1992) and terrestrial Light Detection and Ranging (LiDAR) measurements of spatial distribution of shoots in crown from study sites were used to reconstruct skeletons and foliage distribution of spruce trees in this study.

3.2.2 Field measurements of biochemical and biophysical properties

The forest stand optical, biochemical and biophysical properties, particularly leaf chlorophyll a+b content (Cab) and LAI that were used mainly for validation of retrievals from satellite multispectral images in 2016, were collected in September 2006 and in August 2016 (the peak) of the vegetation seasons. As such, they are compatible with airborne hyperspectral images acquired on the 14th September 2006 (Section 3.2.3) and Sentinel-2 (S2) multispectral sensor image acquired on 31th August 2016 (Section 3.2.3).

3.2.3 Remote Sensing data

Hyperspectral airborne data used in this study were acquired at the Bílý Kříž (Figure 3.1) with the AISA Eagle imaging system (Specim Inc.) during the peak of vegetation season 2006.

The space-born data used in this study to estimate quantitative biochemical and biophysical vegetation parameters were acquired with the multispectral images on board of the EC Copernicus satellite system called S2 (Figure 3.2). The satellite is a part of the Sentinel mission series operated by the European Space Agency (ESA, <http://www.esa.int/ESA>). The multispectral satellite data at the Bílý Kříž site were acquired simultaneously with collection of field biochemical and biophysical properties (31th August 2016).

3.3 Reconstruction of virtual Norway spruce 3D tree models

The first goal of this study was to create realistic digital 3D model of N. spruce tree. There are several approaches that can be applied to create a virtual 3D spruce model, i.e. using simple geometrical primitives or complex 3D shapes. For the radiative transfer modelling purpose of this study was necessary to construct as much precise geometrical model as feasible in order to obtain a benchmark spruce model. Since the input vegetation parameters were only for the Bílý Kříž research site (Section 3.2.2), the constructed 3D spruce models were tailored to this location and data from the Černá hora site were adapted for it.

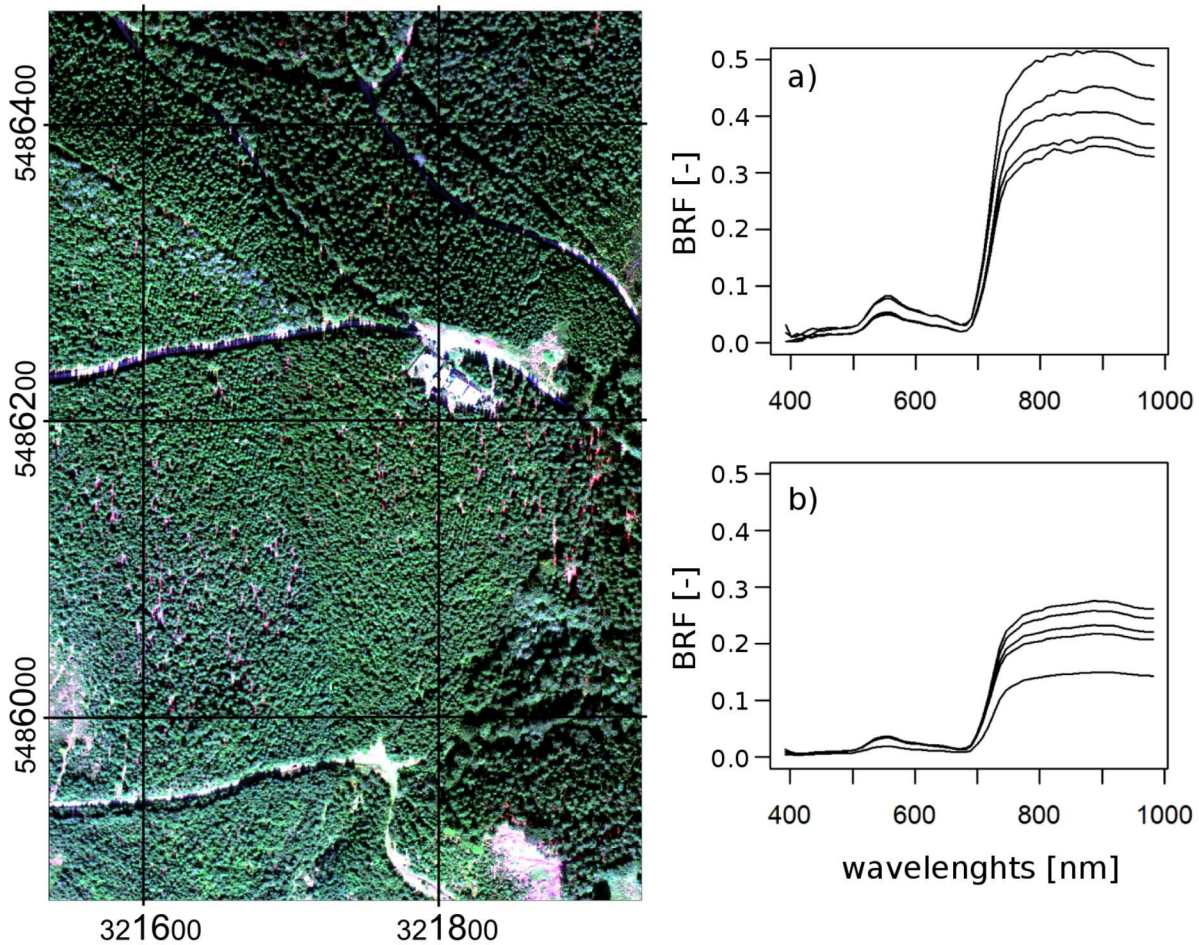


Figure 3.1: Georeferenced RGB composite in natural colors for the AISA Eagle hyperspectral image of the Bílý Kříž site acquired in 2006 (spatial resolution of 0.4 m, 65 spectral bands with spectral sampling distance of about 9 nm projected in UTM Zone 34N (WGS 84)). The right graphs show spectral reflectance signatures of five randomly selected a) spruce crowns and b) aggregated areas of 20 x 20 m (adopted from Homolová et al. 2015a).

The approach used a LiDAR scanning data supplies explicit information about position and density of wood and foliage elements, and combine it with a priori information about angular shoot distribution. Such approach produces 3D digital models of trees based on specifics of the exact location.

Creation of the 3D spruce spruce models was split into three steps.

1. An existing algorithm (Sloup 2013) for spatial reconstruction of trunk and branches from terrestrial LiDAR data was applied (Figure 3.3b, 3.3c).
2. We scaled and transformed the foliage point cloud and wooden skeleton of the spruce model to fit the desired dimensions. It was necessary because the LiDAR data were taken at the Černá hora site, where trees were older and higher, therefore the point clouds had to be scaled the forest dimensions at the Bílý Kříž site.
3. a new algorithm for the distribution of shoots into the tree crown was developed and applied (Figure 3.3e). This last step is crucial and the most innovative achievement of this thesis.

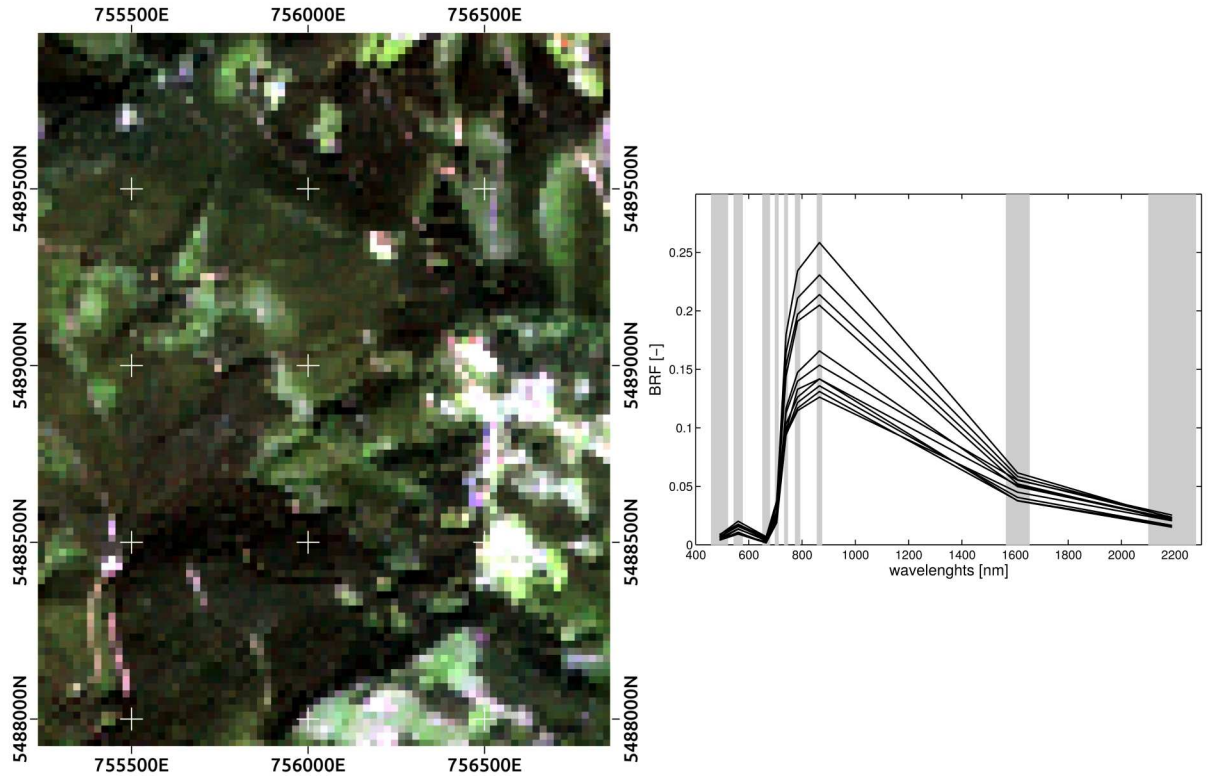


Figure 3.2: Atmosphericly corrected subset of S2 multispectral image for the Bílý Kříž site in natural colors. The image spatial resolution is 20 m and was placed in UTM Zone 33N (WGS 84). The graph at the right hand side illustrates spectral reflectance signatures of eleven randomly selected pixels.

3.3.1 Reconstruction of wooden skeletons - trunks and main branches

In the first step, the algorithm designed by Sloup (2013) was applied to create a detailed wooden skeleton (trunks and main branches) from input terrestrial LiDAR data.

The fully automated algorithm for reconstruction of wooden skeleton is able to process wooden point cloud containing spatial gaps from omission of laser returns due to various obstacles (other branches, trunks, and needles). The process goes in three steps:

1. component identification - spatially-related clusters of the points are identified
2. component analysis - branch structure is reconstructed in each identified component
3. component connecting - all the components are interconnected to form the final branch structure (Sloup et al. 2013)

The process of connecting the components together was designed to keep real architecture of branches and their connections to the trunk (Figure 3.3c).

3.3.2 Translation and scaling of the foliage point cloud

The second step was needed to translate spatially the foliage point cloud in such a way it matches the virtually reconstructed wooden skeleton and subsequently to scale them both to fit the desired dimensions at the Bílý Kříž site.

The output of the first step, i.e. The reconstructed 3D wooden skeleton, was created in local coordinate system with origin in the center of the trunk base. To ensure the same

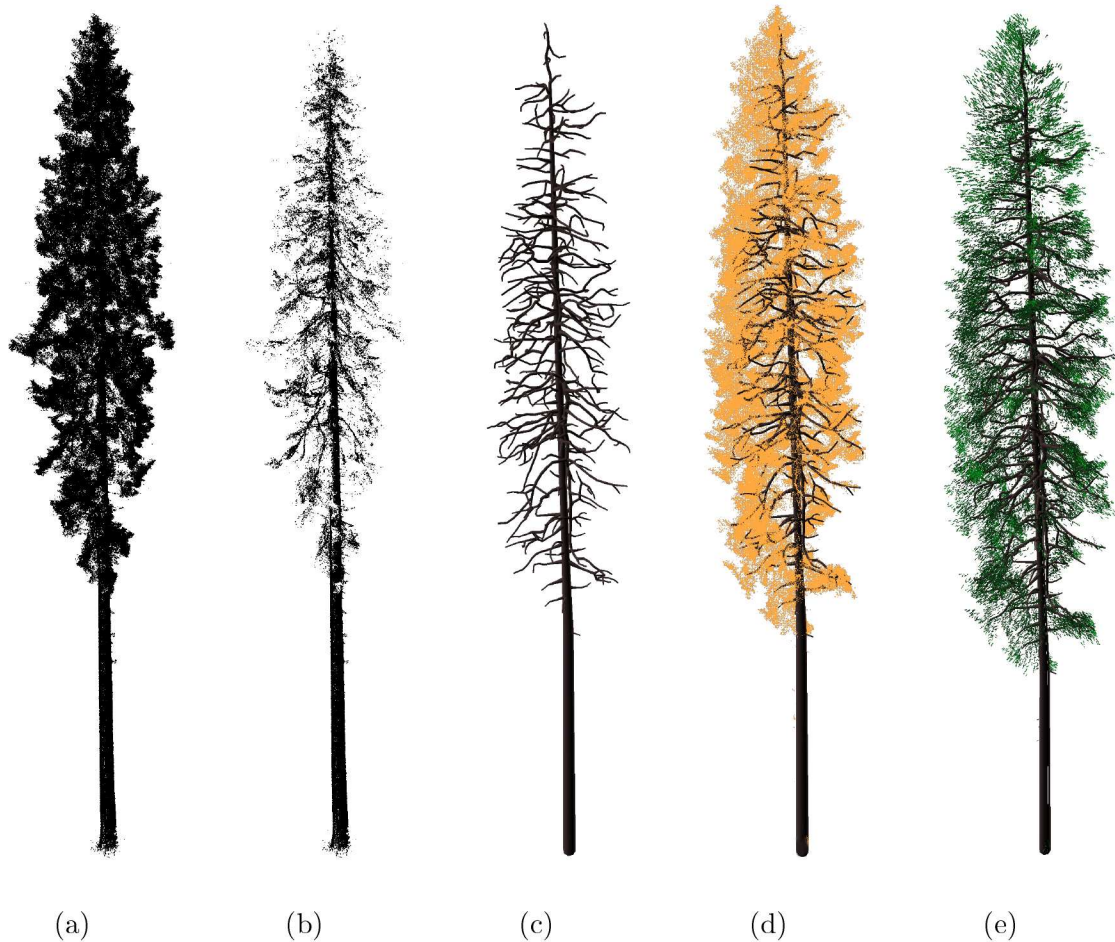


Figure 3.3: Creation of a virtual 3D spruce model from a terrestrial LiDAR point cloud. a) original terrestrial LiDAR scan of a spruce tree (Section 3.2.1), b) separated wooden point cloud (Section 3.2.1), c) reconstructed wooden skeleton (Section 3.3.1), d) reconstructed wooden skeleton with scaled foliage point cloud (Section 3.3.2), and e) the final 3D spruce model populated by shoots of two age categories: current year (light green) and older shoots (dark green) (Section 3.3.3).

coordinates as for wooden skeleton, the foliage point cloud was spatially translated according its coordinates system.

As already mentioned the terrestrial LiDAR scans were acquired at the Černá hora site, whereas estimation of forest quantitative parameters was performed for the Bílý Kříž site, where airborne, satellite, and field data were available all together (Sections 3.2.2 and 3.2.3). Since spruces at the Černá hora site were older and higher than trees at the Bílý Kříž site (Section 3.1) a scale transformation was needed to equalize foliage point clouds with size of reconstructed wooden skeletons in order to fit dimensions of trees at the Bílý Kříž site.

After transforming the foliage point cloud according to the wooden skeleton, the algorithm distributing shoots within a crown can be applied based on the transformed foliage point cloud.

3.3.3 Algorithm for shoot distribution within spruce crown

The last step in the process of the 3D spruce model creation was distribution of shoots within crown. Spatial distribution of needles has significant impact on the light scattering, especially in the near infrared (NIR) part of the electromagnetic spectra. Consequently, the dis-

tribution of shoots of different age categories is crucial part of the whole 3D spruce model reconstruction. Shoot distribution must reflect the actual foliage point cloud establishment (Section 3.2.1), existing leaf density and geometry expressed in the form of the LAI and leaf angle distribution (LAD). The algorithm for shoot distribution uses information about shoot positions from foliage point cloud (Section 3.2.1), about shoot density from the LAI (user defined variable), and about angular distribution from LAD obtained from Barták (1992, Section 3.2.1).

The LAI is required to be retrievable as a free variable. It has to be parametrized independently. In other words, the model is constructed based on user predefined value of the LAI.

Shoots are defined as separate 3D objects (i.e. planes along the shoot axis, individual needles), however for the description of this algorithm it is not important to consider the exact shoot representation (Section 3.4.2).

The shoot distribution procedure had three main steps. In the first step we calculate the position of each shoot within a tree crown. In the second step we split shoot positions in two groups by their age: current-year shoots and older shoots. Finally, in the third step we place shoots to their defined spatio-geometric positions and angular orientations.

Calculation of shoot positions

As already indicated, the number of shoots depends on the user-defined LAI. The total number of shoots within a reconstructed crown is, therefore, computed from a given LAI value.

The calculation of shoot positions runs in two steps. First, we separate the foliage point cloud into cubes with a given size (side around 0.18 m for trees of 15 m in height). The size of cubes directly influences the computational time because more points present in a single cube requires more time to calculate all shoot positions. Thus, the size of cubes is expected to be specified by the user according to available computational resources and density of processed foliage point cloud.

In the second step we calculate shoot positions within every cube. The positions are calculated by k-means function from the cluster analysis theory. Each cube contains set of points $\mathbf{x} = \{\mathbf{x}_1, \mathbf{x}_2, \dots, \mathbf{x}_n\}$, where $n \in \mathbb{N}$ is a number of the points in the currently processed cube. Each point is defined by its position $\mathbf{x}_i = (x, y, z)$. The k-mean clustering makes a partition in the set of points into the $k < n$ subsets $\mathbf{S} = \{S_1, S_2, \dots, S_k\}$. The k is then calculated from the given number of shoots:

$$k = \frac{n}{\frac{n_{points}}{n_{shoots}}}, \quad (3.1)$$

where n_{points} is number of total points in the whole foliage point cloud. The k-mean function provide also coordinates of the clusters centroid, which represents the position, where a shoot is placed. The algorithm iterates through all cubes with at least one point defines position of each shoot.

Separation of shoots in two age categories

Next task is to extract shoot positions of two needle age groups: current-year and older needles (Figure 3.3e). For this we divide the processed tree into the cubes with a different size. It would be possible to use the original cubes, established during the calculation of the shoot positions, but since the new cubes do not need to be so small, their larger size helps us to save computer memory and computational time. Nevertheless, creation of both cube meshes requires per tree optimization, because each tree varies in size and structure and also it has

LiDAR scans of different quality in sense of point density, number and size of gaps etc. Therefore, size of cubes for the shoot location calculation is generally smaller (in our case 0.18 m), whereas cubes for the shoot separation into the age categories are larger (in this study 0.3 m for 15 m high trees).

Before we start separating the needle shoots into two age categories, we need to find a tree envelope, i.e. cubes at the tree crown's periphery, where the current shoots occur prevalingly at the crown periphery. The process of finding the crown envelope consists of four steps (illustrated in Figure 3.4):

The crown envelope convexity reduction prevents the new shoots are being placed inside the crown as they are naturally growing at the periphery. This may happen when the air gap size is larger than cube size. The following steps were implemented to reduce the inappropriate crown envelope convexity (illustrated in Figure 3.5).

The algorithm processes tree crown, as being divided in several horizontal layers (l_n). The height of each layer is based on empirical observations that one whorl takes about 0.8 m of crown height. The percentage of the current-year needle category in each layer was assigned according to measurements published by Barták (1992). The following steps were carried out (illustrated in Figure 3.6).

Shoots transformation to their position

Once the position of all shoots are determined, shoots are distributed within a tree crown. The shoots have to be first rotated and then translated depending on their position in tree crown. Transformation matrix for these two-step operation is calculated for each shoot separately. For the transformation composition it was more efficient to apply first the rotation and then the translation.

A shoot was first rotated around the y and z axis. The elevation angle was assigned according to measurements published by Barták (1992). The calculation of the azimuth angle γ is based on l_x and l_y . It is randomized by an angle ψ gaining values within the range $\langle -\frac{\pi}{4}, \frac{\pi}{4} \rangle$. The vector for shoot translation was then calculated as $\mathbf{v} = (L - \mathbf{0})$, where $\mathbf{0}$ is the origin of the coordinate system.

3.3.4 Main outcome

New 3D model of a Norway spruce tree reconstructed from terrestrial LiDAR scans is the main outcome of this part. The 3D model is composed out of two sets of objects created separately: wooden skeleton and foliage - needle shoots. The wooden skeleton was reconstructed using LiDAR returns from main wooden tree parts (trunk and branches) with the algorithm designed by Sloup (2013). The foliage reconstruction was done with a new algorithm designed in this study. The main task of this algorithm is biologically correct distribution of shoots within a tree crown, which represents the most innovative outcome.

The reconstructed 3D spruce model of a single tree contains significantly large number of facets, about 22 Millions. For better imagination, the same number of geometrical facets was needed to create a large scale 3D representation of Toulouse city center in France. In order to achieve a feasible computational time, it was necessary to optimize the model before its operational use for simulating canopy forest scenes in the DART model. The optimization procedure is described in the following Sections 3.4.2, 3.4.3, and 3.4.4.

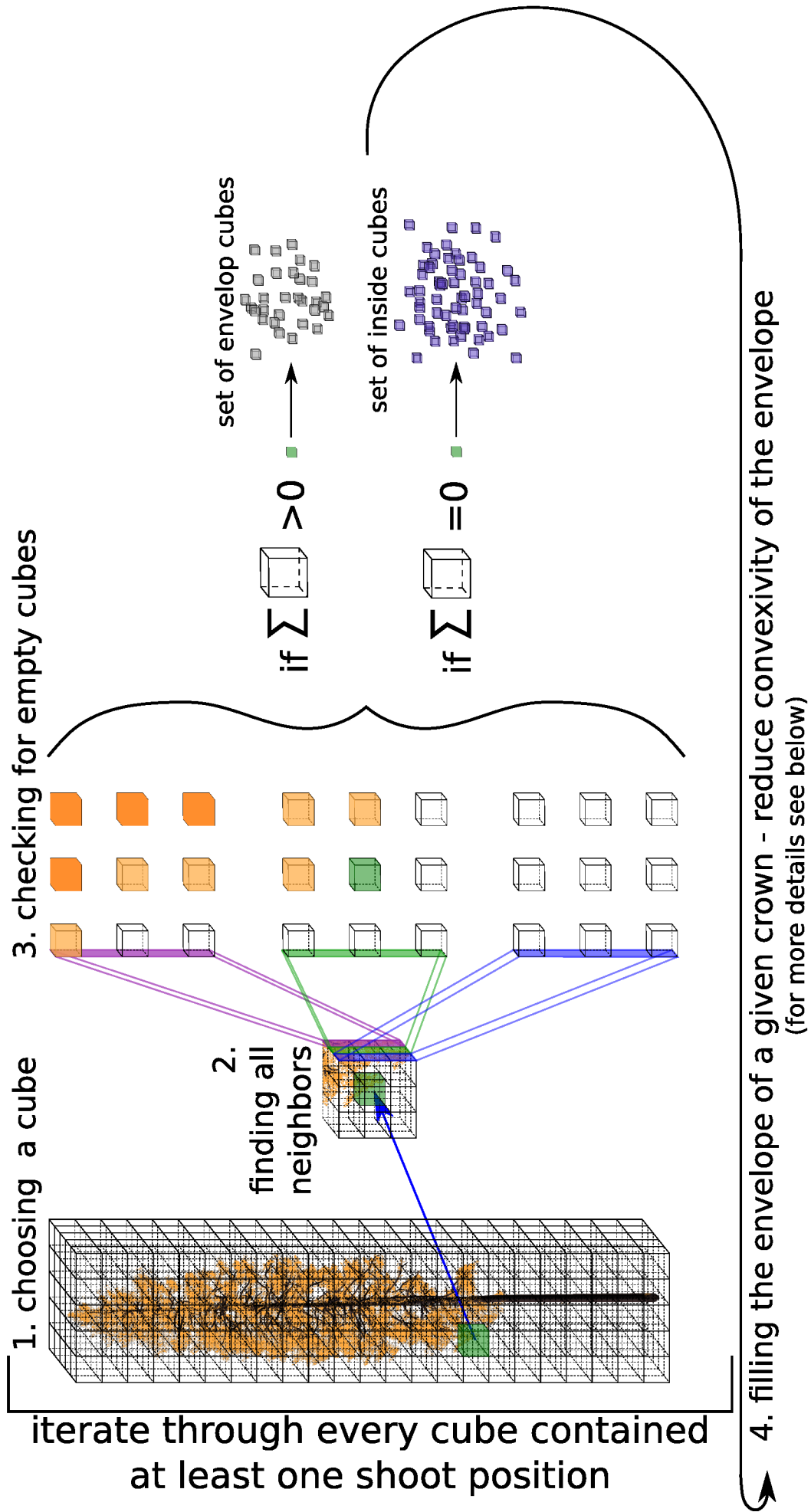


Figure 3.4: The process of finding crown envelope.

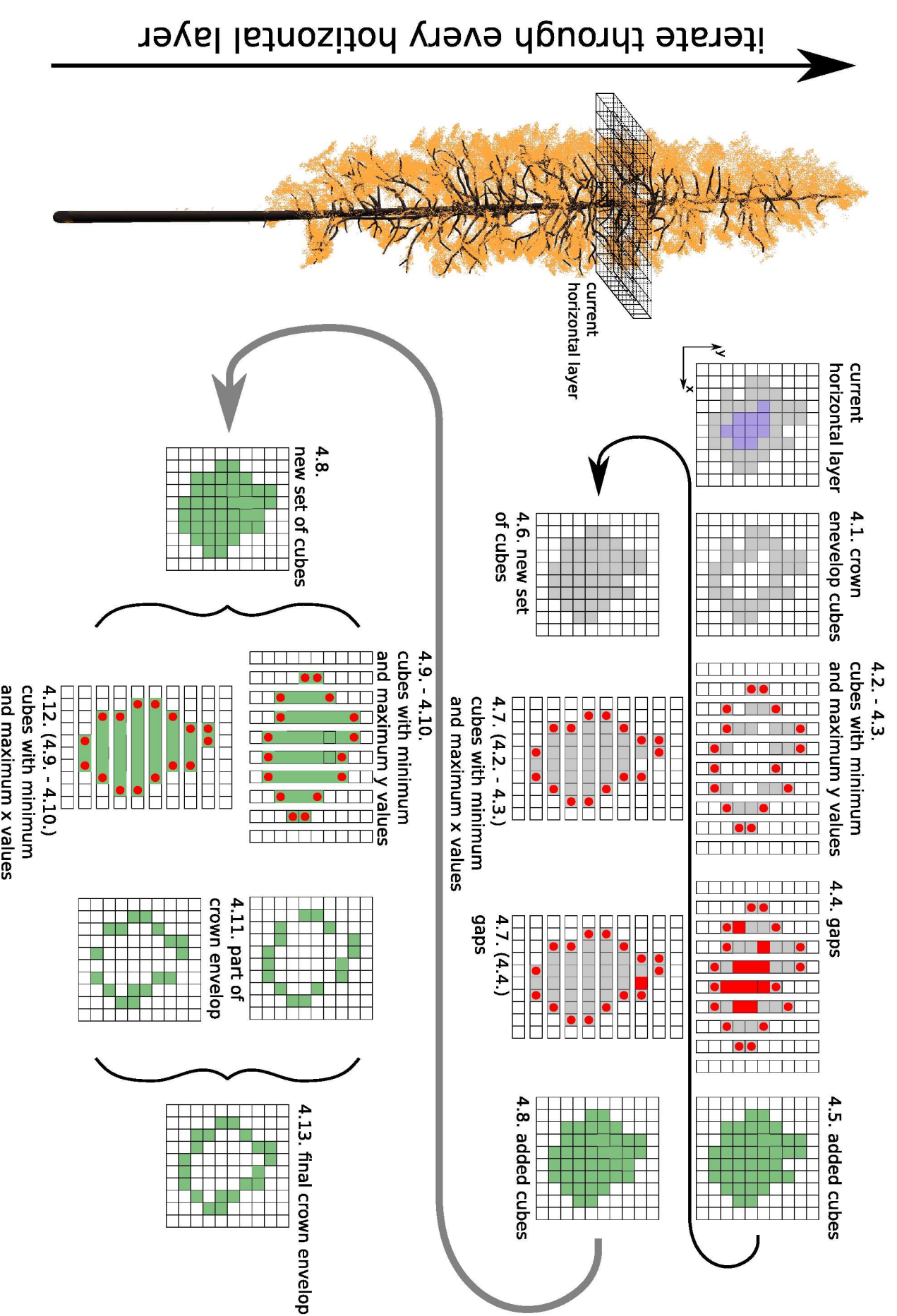


Figure 3.5: The process of crown envelop convexity reduction. This process describes in a detail the step 4. that forms the process of finding crown envelop.

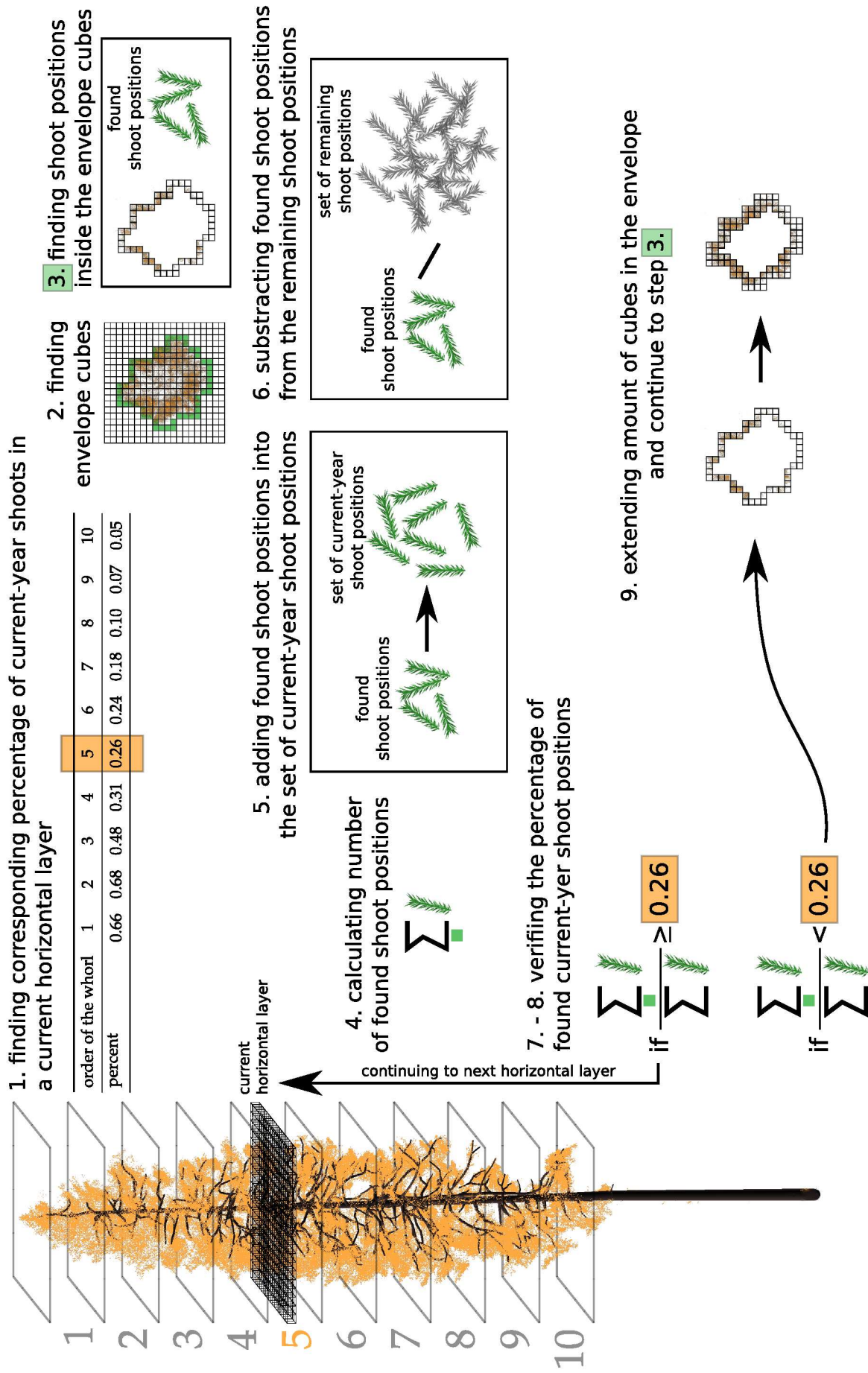


Figure 3.6: The process of separating finding crown envelope. The process iterates through every cube one by one, where are some points from foliage point cloud.

3.4 Radiative transfer modeling and optimization

One of the main goals of this thesis was to optimize 3D spruce model that it is applicable for radiative transfer (RT) simulations. Radiative transfer of forest scenes composed from the 3D spruce models with needle shoots (Figure 3.9a) contain large number of facets, therefore RT computation is extremely demanding. For the operational use, it is necessary to optimize the scene parametrization.

This section is separated into four parts. The first part describes all possibilities how to parametrize trees in the DART model (Section 3.4.1). The last three parts describe the optimization that was studied at three structural levels:

shoot level: Four shoot models were evaluated (Section 3.4.2),

tree level: Four shoot models were evaluated in whole tree and compared to airborne data (Section 3.4.3),

canopy level: Four shoot models were evaluated in whole forest scene and compared to airborne data. The 3D spruce models were transformed to turbid cells (Section 3.4.4).

3.4.1 DART scenes

In the DART model it is possible to parametrize trees in several ways (Figure 3.7). The first way uses the pre-prepared geometric crown shapes (base model) (Figure 3.7 on the right). Turbid cells contain infinite number of infinite small facets, which are distributed in the cell based on LAD, LAI and other DART parameters specifying gaps distribution in the tree crown vertically and horizontally. The tree crown can be separated into horizontal levels and for each level it is possible to set up different properties of turbid cells, gaps distribution and relative trunk width. The base tree models are used mainly because they reduce computation requirement. However, for coniferous trees this parametrization may leads to large discrepancies in forest reflectance simulations. The difference between DART simulated and remote sensing (RS) reflectance is illustrated in Figure 3.8. From the comparison it can be seen that more significant differences are found for the coniferous spruce stand than for broadleaf beech stand. The possible explanation is that the base tree model is not able to describe fine scale scattering properties of conifer trees.

The second way how to parametrize trees in the DART model is to import a 3D tree model (Figure 3.7 on the left). This approach allows to import object groups and set up different properties to each group, e.g. set up different optical properties for different age category of shoots.

The 3D tree model can be treated in two different ways. First radiative transfer is calculated directly on the 3D model. This approach is very precise, but extremely computationally demanding. Simulating a scene with several mature trees is almost impossible.

The second way how to treat the 3D tree model is to transform the foliage part to turbid cells. This approach preserves the structure of the tree and the distribution of the foliage within the tree crown. The possibility to set up different optical properties for different object groups is also preserved. Although RT computation is slightly more demanding than for the base model with predefined crown shapes, it produces more accurate simulations of canopy reflectance.

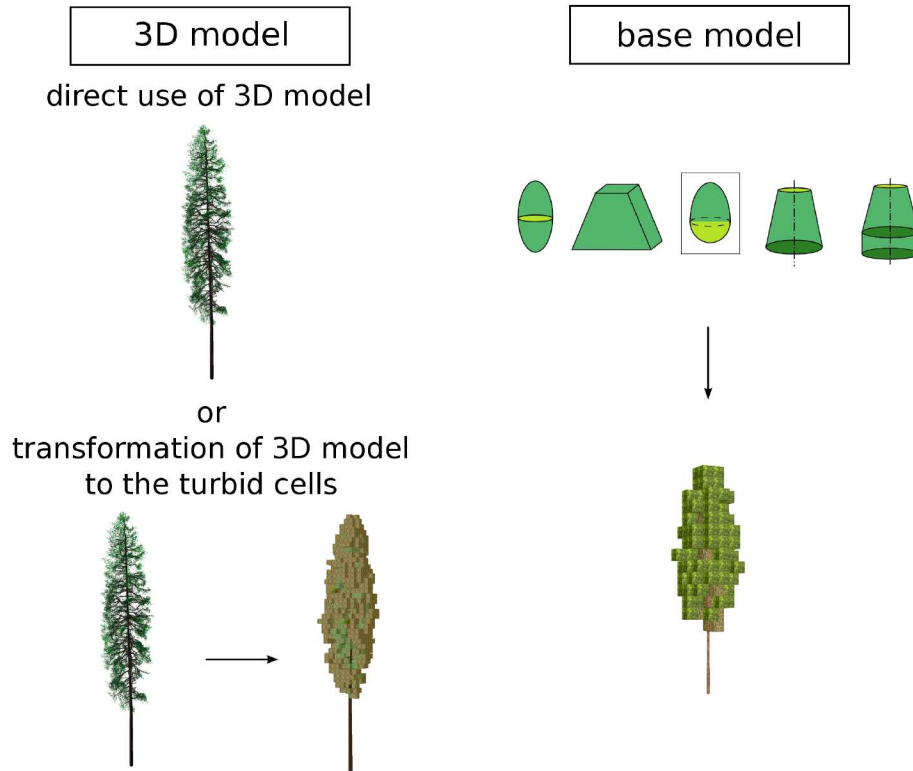


Figure 3.7: There are three ways how to parametrize trees in DART: using 3D tree model directly, letting 3D tree model to be transformed to turbid cells, and using trees with pre-prepared geometric crown shapes (base model).

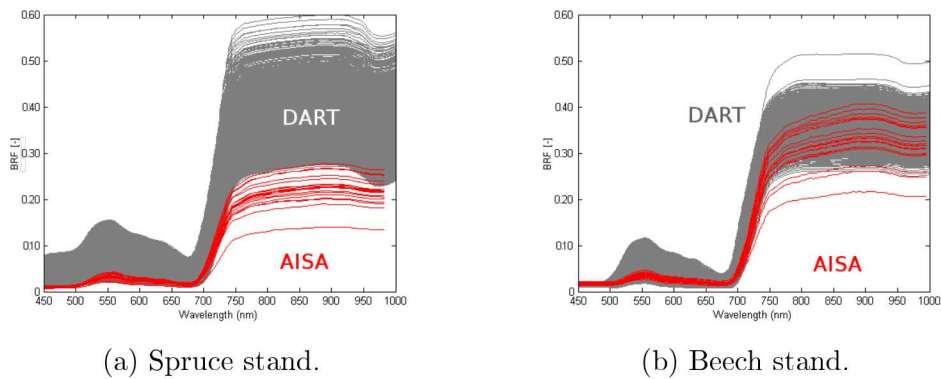
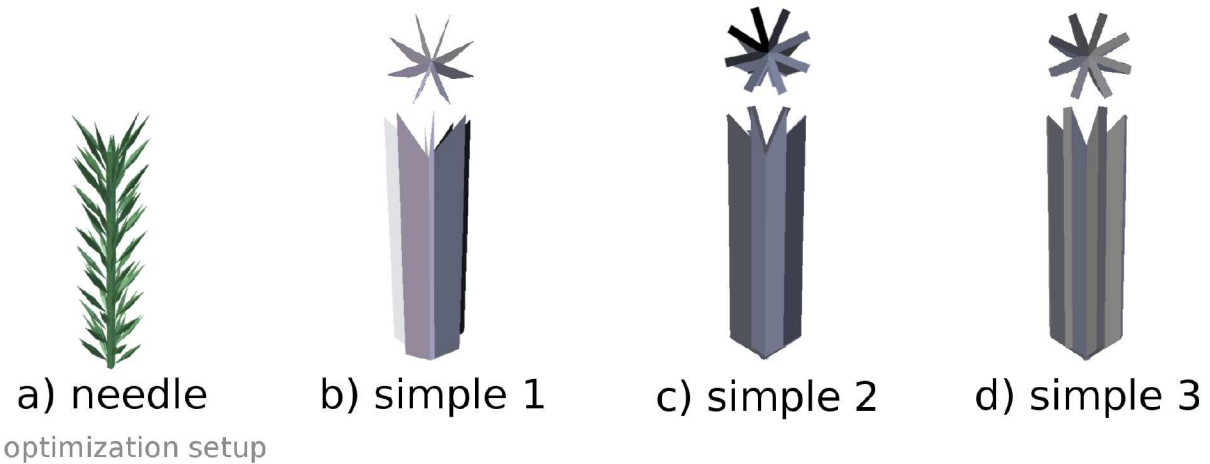


Figure 3.8: A comparison of spectral reflectance between results simulated by with base spruce model (grey) and airborne data (aggregated into 20 m pixel size) acquired by the AISA Eagle imaging system (red).

3.4.2 Optimization at shoot level

Objectives of this part were:

- to find the optimal DART parametrization of the reference 3D needle shoot model (Figure 3.9a) and to find the best 3D simplified shoot model (Figure 3.9b)
- to compare these two shoot models with optimal distribution of sun zenith and azimuth angles.



2 ground reflectances (0, 1), 3 viewing angles, 5 cell sizes

Figure 3.9: Model of a spruce needle shoot (needle) a) and its simplifications b)-d). The first simplified model (simple 1) b) is created by adding planes along the shoot axis and the area of the needles are the same as the planes. The second simplified model (simple 2) c) is created by adding small perpendicular plane on top and bottom of each plane from the first simplified model b). The third simplified model (simple 3) d) is created by adding a width dimension to the planes from the first simplified model. The width corresponds to the size of the small perpendicular planes from the second simplified model c). The optimization setup is shown at the bottom of the figure.

3.4.3 Optimization at tree level

The main objectives of this optimization were:

- to compare shoot models at the tree level,
- to compare angular dependency at the tree level with the results at the shoot level,
- to compare DART simulations of:
 - 3D spruce model with needle shoot model,
 - 3D spruce model with simple 1 shoot model,
 - base spruce model,
 - 3D spruce model with needle shoot model transformed to turbid cells,
 - 3D spruce model with simple 1 shoot model transformed to turbid cells, and
 - airborne image.

3.4.4 Optimization at canopy level

The previous two optimizations at the shoot and the tree levels were useful to assess the quality of the 3D tree model and its simplifications, but for the purpose of estimation of vegetation parameters from RS data it is needed to use the DART model at the canopy level, i.e., a scene with several trees. For the canopy level simulations, however, time and computer requirements need to be carefully considered. The aim of this comparison is to decide, if the transformation to turbid cells yields similar results to the RS data or if it is necessary to use 3D spruce models directly.

At this level of comparison, it was not possible to simulate entire canopy scene using 3D spruce models, because it was too computationally demanding, but the canopy foliage objects had to be transformed to turbid cells. The comparison at this level was done for five DART canopy scenes which were compared with airborne data. The five DART canopy scenes were:

- 3D spruce model with needle shoot transformed to turbid cells,
- 3D spruce model with simple 1 shoot transformed to turbid cells,
- 3D spruce model with simple 2 shoot transformed to turbid cells,
- 3D spruce model with simple 3 shoot transformed to turbid cells, and
- base spruce model.

3.4.5 Main outcome

Since the reconstructed 3D spruce model was too complex for direct implementation in the DART model, the key outcome of this part was the optimized 3D spruce representation.

The optimization at the shoot level used two new simplified shoot models (labeled as simple 2 and simple 3) to replace the detailed reference needle shoot model. A high agreement with the reference was found for the simple 2 shoot model. However, a strong angular dependency was still observed when simulating single shoots, with the largest differences in the nadir viewing angle caused by regular structure of planes in the simplified shoot models. Less angular dependencies were expected at the tree level, because of larger angular variability in distribution of shoot within the crown. Contrary to the shoot level, the optimal solution at the tree level was obtained with the simple 1 shoot model, which yielded slightly better results than the simple 2 model. Results confirmed the angular homogenization of a single tree crown reflectance.

Even if trees are modelled as 3D objects, the computation of radiative transfer in DART is done for discrete cells. The size of those cells controls amount of incident radiation and therefore multiple scattering between the 3D objects. For both 3D spruce models without transformation to turbid cells we observed lower reflectance values compared to the airborne data and spruce models transformed to turbid cells (Figure 3.10). This could be attributed to limited multiple scattering due to too coarse cell size (10 cm) chosen for this comparison. We expect that the finer cell size could produce results closer to real airborne data, but it was unfeasible to compute it in this thesis with the current computer resources.

The goal of the canopy level optimization was to decide, if the 3D spruce models transformed to turbid cells are sufficiently representative for accurate estimations of selected vegetation parameters from RS data. The choice of the optimal tree parametrization was based on comparison of reflectance simulations using all four shoot models (Figure 3.9) with the airborne data of a spruce forest. The results revealed that the 3D spruce model transformed to turbid cells significantly improved forest canopy reflectance simulation (Figure 3.11). This spruce model with the simple 1 shoot model produced simulated reflectance, which, compared to the results obtained with the base spruce model, fits better with real airborne hyperspectral image data. RMSE values calculated between mean of airborne data and DART canopy simulations confirm that spruce model with simple 1 or simple 2 shoot model with RMSE values 0.0106 and 0.0100 fit better to real airborne hyperspectral data than the base spruce model with RMSE value 0.0828.

The outcome of this part is not definite. As the DART model is being constantly updated and its computational efficiency improved, a more efficient 3D spruce model can be defined

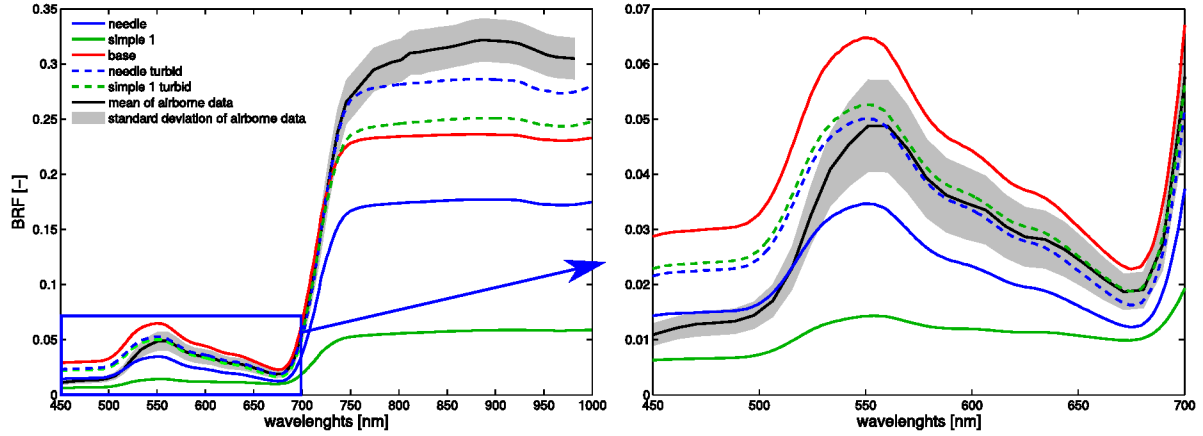


Figure 3.10: Comparison of selected pixels from airborne image data, their mean and standard deviation, with 3D spruce model with needle shoot model (needle), b) 3D spruce model with simple 1 shoot model (simple 1), c) base spruce model (base), d) 3D spruce model with needle shoot model transformed to turbid cells (needle turbid), and e) 3D spruce model with simple 1 shoot model transformed to turbid cells (simple 1 turbid).

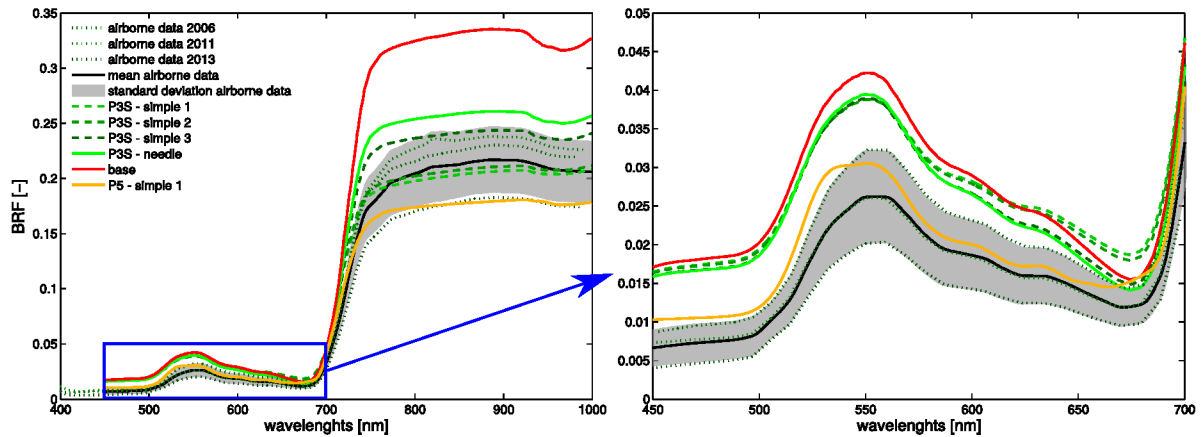


Figure 3.11: Comparison of airborne data and DART simulations with different type of tree parametrization. There are showed three airborne data from years 2006, 2011, and 2013, their mean and standard deviation. DART simulations are with base spruce models, with needle, simple 1, simple 2, and simple 3 shoot model, where optical properties were simulated by PROSPECT 3S (P3S). Last is simulation with simple 1 shoot model but the optical properties were simulated with PROSPECT 5 (P5). On the left side are the spectra, and on the right side are the spectra only in VIS region of the spectra.

in a near future. It is expected that the computation efficiency of the DART model will soon allow to simulate canopy scenes created from geometrical objects without the turbid cell transformation necessity.

3.5 Estimation of quantitative vegetation parameters

The main goal of this study was to test if the optimized 3D spruce model improves the estimation of vegetation parameters (i.e. Leaf chlorophyll a+b content (C_{ab}) and LAI) from satellite observations. In order to assess the improvement, the vegetation parameters were estimated

by two look-up tables (LUTs), which were generated by two parameterizations of spruce canopy in the DART model (base versus 3D spruce model). The first parameterization of the spruce canopy was based on the base spruce model, the second parameterization was based on the optimized 3D spruce model (described in Sections 3.4.2, 3.4.3, and 3.4.4).

This section is composed of three parts:

- Creation of the two types of LUTs (Section 3.5.1).
- the retrieval of vegetation parameters from Sentinel-2 (S2) images by applying support vector machines (SVM) to both LUTs and necessary optimization of the SVM input parameters (Section 3.5.2).
- Last, validation of estimated parameters with the field data acquired at the Bílý Kříž site (Section 3.5.3). The last step helped to evaluate the impact of 3D spruce model and its DART parameterization, which was newly developed in this thesis.

3.5.1 LUT creation

The LUTs were created within the framework of two international projects (RedEdge - RED-EDGE-CG-CESBIO-ATBD-03-0002 and HYPOS - AO/1-8345/15/NL/LvH projects, European Space Agency), therefore they differed based on project specifications such as in spruce model parameterization, LUT structure, version of the DART model used for its creation etc. The LUT with the base spruce model was tailored to airborne and field data from the Bílý Kříž site in 2006 (see Sections 3.2.2 and 3.2.3). The LUT with the 3D spruce model transformed to turbid cells was tailored to satellite and field data at the same study site, but in 2016 (see Sections 3.2.2 and 3.2.3). For LUTs creation the newest version of the DART model available at the time when they were simulated was used. Some improvements of the DART model were specifically made for the purpose of these projects. Most of improvements are made in sense of computation efficiency.

Base spruce model

These LUT simulations were made with the DART model version 5.5.1 v494 (released in 2014). In the following paragraphs only the variable parameters of the DART scene will be described and they are summarized in Table 3.1.

parameters	base model	3D model
canopy cover (CC)	50, 65, 80, 95 %	
LAI	3 – 10 with step 1	
topography (topo)	flat, south, north, and east slope	
leaf optical properties (lop)	900	464*

Table 3.1: Structure of DART simulated spectral database. (*) *leaf optical properties in case simulations with 3D spruce models are generated together with the LAI values. That means, for each case of generated leaf optical property was randomly chosen the LAI value from range 3 – 10. Instead of the case of simulations with base spruce models they were generated set of leaf optical properties and this set were assigned to each LAI level.*

Leaf optical properties that were used as inputs into the DART model were simulated using PROSPECT 3S, which was specifically adjusted for the Norway spruce needles by Malenovský et al. (2006). In case of the base spruce model DART is able to separate the tree crown in horizontal layers, therefore the leaf optical properties were defined for three crown levels (exposed, transition, and shaded).

Meaningful combinations of PROSPECT input parameters were randomly derived using the Matlab function `mvnrnd`, which generates multivariate normal random values. This function takes into account covariance computed among the measured PROSPECT input parameters. The function generated an initial pool of 50 000 input combinations that were restricted by realistic min – max ranges defined according to available literature (Stuckens et al. 2011, Feret et al. 2008, 2011, and Ciganda et al. 2009) or by available experimental measurements.

Since one of the estimated parameters is C_{ab} , it was essential to ensure that the sampling space of possible chlorophyll values was spaced equally. Therefore, the initial pool of input combinations was divided into equally spaced groups of C_{ab} values (e.g. C_{ab} varied between 10 and 100 $\mu g cm^{-2}$, we obtained nine groups representing nine intervals of 10 $\mu g cm^{-2}$ each). From each group ten PROSPECT input combinations were then randomly selected resulting in 900 combinations scenes.

3D spruce model

These LUT simulations were made with the DART model version 5.6.3 v858 (released in 2016). The setup this LUT structure is almost similar to the previous one with base spruce model, the major difference is in simulation of input optical properties and distribution of the LAI (Table 3.1). The optical properties were simulated using the PROSPECT 5 RTM (Jacquemoud and Baret 1990; Feret et al 2008).

Needles of spruce trees were divided into two categories, current-year needles growing at crown periphery (20 %) and older needles growing inside the crown (80 %) (Section 3.3.3). The older needles generally have higher C_{ab} , carotenoid (C_{ar}) and dry matter (C_m) content (Homolová et al. 2013) and this was reflected in the distribution of PROSPECT 5 input parameters.

Other difference is in the distribution of the LAI. In the case of simulations with the base spruce model generated set of leaf optical properties were assigned to each LAI level. But in case of simulations with the 3D spruce model the LAI values were randomly chosen from the range 3 – 10 and assigned to each generated leaf optical properties. That enabled a smaller size of the LUT.

3.5.2 Estimation of C_{ab} and LAI

The C_{ab} and LAI retrievals were implemented using SVM (Chang & Lin 2011), as these algorithms represent a good compromise between computation cost, efficiency and accuracy. SVM are kernel-based computer learning algorithms used widely for solving N-class classifications or regression problems (Smola & Schölkopf 2004).

The SVM was trained with 1000 samples and applied on S2 image data for both cases of LUT. For better visualization the results of the estimated C_{ab} and LAI were displayed in discrete ranges (according to expected real values). Therefore the pixels with extreme values were not classified. Final maps of estimated C_{ab} and LAI from both LUTs are shown in Figures 3.12 and 3.13.

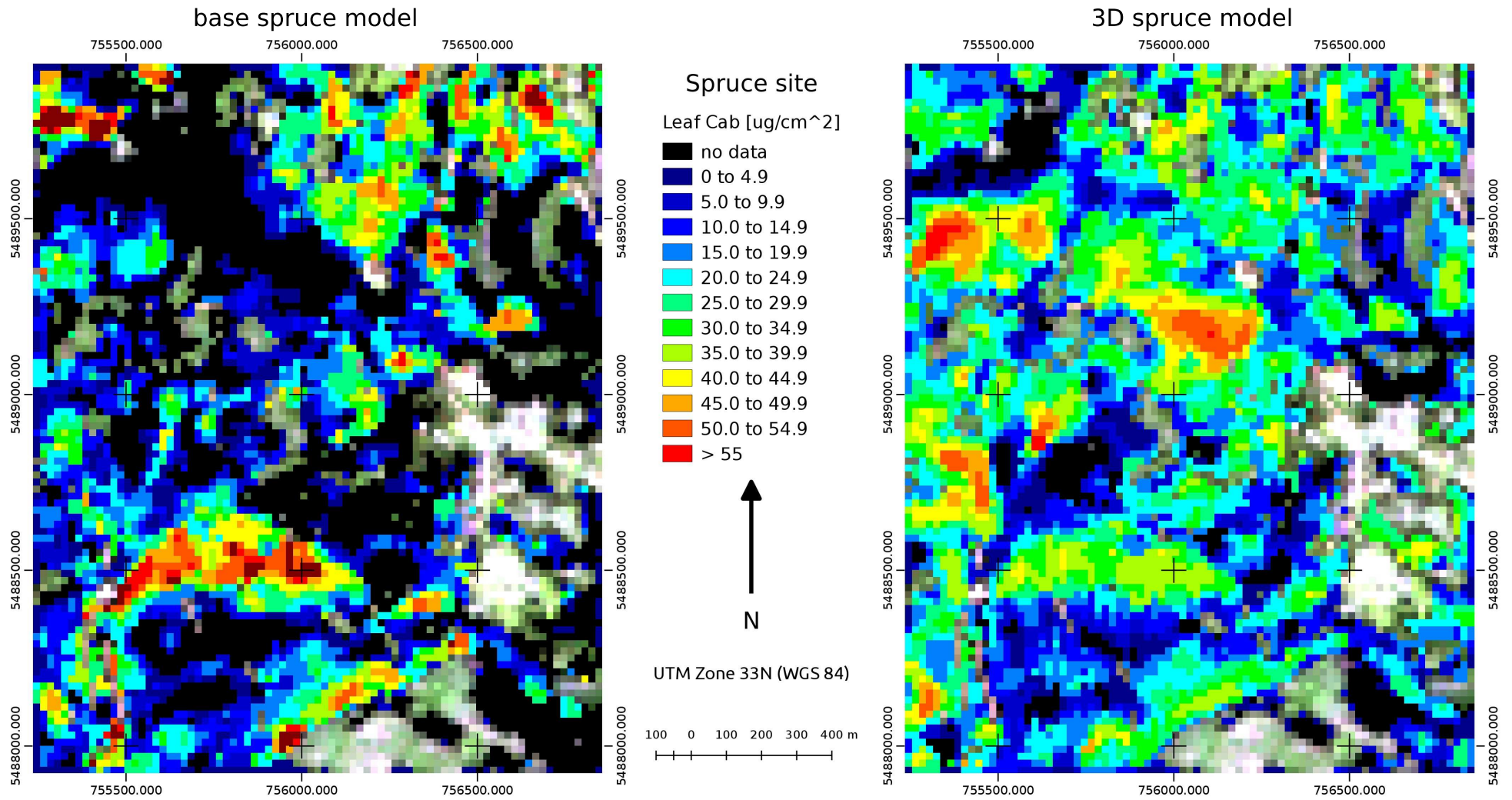


Figure 3.12: Estimated Cab content. The map on the left was calculated from LUT with base spruce models, the map on the right was calculated from LUT with 3D spruce models transformed to turbid cells.

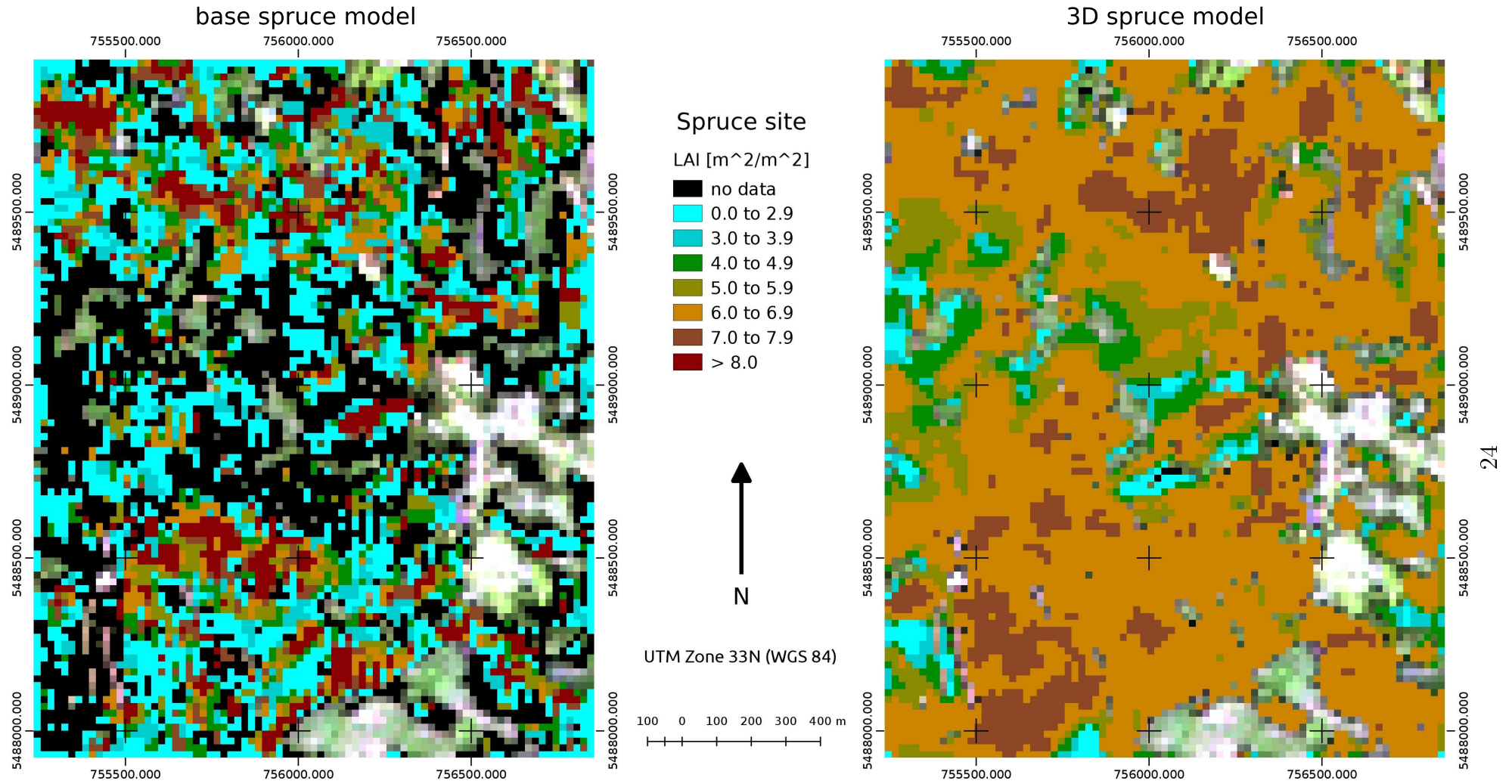


Figure 3.13: Estimated LAI. The map on the left was calculated from LUT with base spruce models, the map on the right was calculated from LUT with 3D spruce models transformed to turbid cells.

3.5.3 Validation against the field data

Validation of the Cab and the LAI retrievals from S2 images were done with the field data that were measured almost synchronously with S2 acquisition in summer 2016 (see Section 3.2.2).

For validation of estimated Cab from S2 images with the pixel size of 20×20 m, there are only seven values available. The number is very low, since gathering of this type of data is very time consuming. The validation was realized as a scatter plot between the measured and estimated values (Figure 3.14). Furthermore, RMSE values were computed for all combinations of parameters and used spruce models.

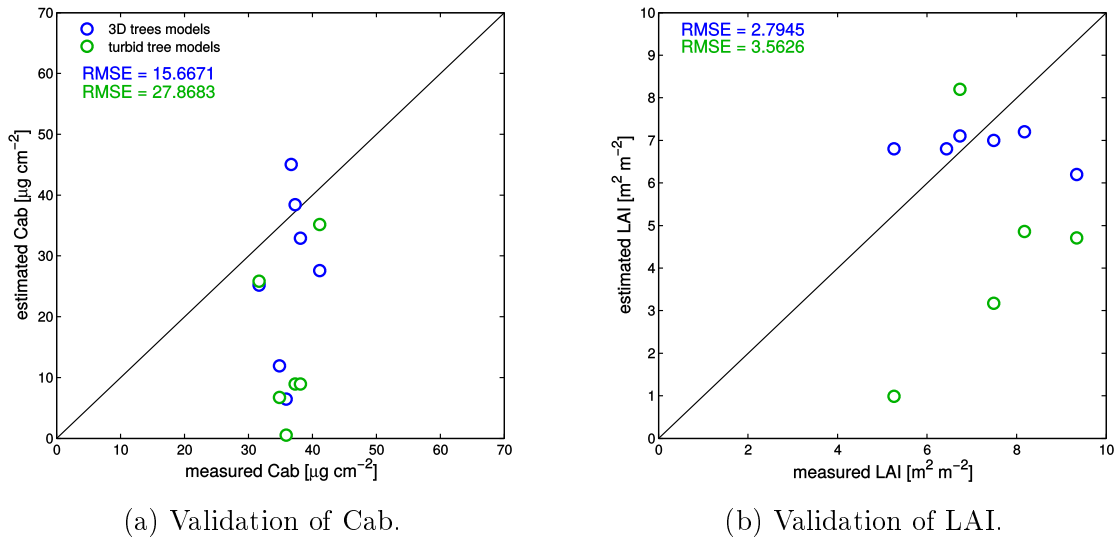


Figure 3.14: Validation of the estimated Cab and LAI values from S2 images of seven localities at the Bílý Kříž site. In graphs are two sets of data depends on 3Dvspruce models used for generation of the LUT. First are used 3D spruce models transformed to turbid cells (blue) and second are used the base spruce models (green). There are also calculated RMSE value for both cases and both parameters.

From the RMSE values can be seen that the retrievals with the 3D spruce model are closer to the field data than the case with the base spruce model. In case of the Cab estimation the RMSE decreased from $27.9 \mu\text{g cm}^{-2}$ to $15.7 \mu\text{g cm}^{-2}$, in case of LAI it decreased from $3.5 \text{ m}^2 \text{m}^{-2}$ to $2.8 \text{ m}^2 \text{m}^{-2}$ because of implementing the 3D spruce model. Regarding the spatial patterns, the Cab map derived from the 3D spruce model exhibits realistic pattern, whereas the maps derived from the base spruce model has high number of negative values. The LAI map derived from the 3D spruce model also exhibits more realistic pattern than the map derived from the base spruce model, where values seems to be distributed randomly. Despite this, the estimated LAI derived from the 3D spruce model does not capture the variability as observed in the field data. The possible explanation is that the variability of LAI in the LUT with the 3D spruce model is not sufficient and the SVM method is not able to cope with that fact.

3.5.4 Main outcome

The last aim of this study was to assess the improvement achieved in the remote sensing estimation of the two vegetation parameters, Cab and LAI, after operational implementation of the newly designed 3D spruce model. The validation against field data of both canopy traits estimated using the base and the 3D spruce models was performed. Results showed that the accuracy of both parameters retrieved from a Sentinel-2 multispectral image was improved when the precise 3D spruce model transformed into the turbid cell representation was implemented instead of the traditional DART turbid tree model. The improvement was clearly observed in a higher consistency of spatial patterns in both Cab and LAI maps.

Nevertheless, the direct comparison with the field data suggests that there is still a room for further improvements. For example, the application of the Sentinel-2 image topographic correction, which was not available during this study, would decrease the angular anisotropy of a spruce canopy reflectance. This correction removes canopy reflectance differences especially on steeper slopes of different expositions (northern vs. southern slopes), which would reduce mathematical illpostness of the retrievals and consequently increase their accuracies. Other potential improvement could be a meaningful restriction of the DART simulated LUT based on a prior knowledge, such as known topography, canopy covers and/or a reasonable limitation of ranges of free (searched) variables (Cab and LAI). This approach would, however, require production of more specialized DART LUTs applicable to specific forest types. The retrieval would require pre-classification and segmentation of the satellite image into the corresponding forest type classes. It should be mentioned, that misclassified forest types coupled during the retrieval process with an inappropriate LUT could potentially result in even higher errors than current approach.

4 | Synthesis and outlook

4.1 Main conclusions and impact

The detailed computer 3D model of Norway spruce tree, based on reconstruction of terrestrial LiDAR point clouds, was successfully created. A new algorithm was developed for biologically correct distribution of the needle shoots within the reconstructed tree crowns. Optimization of the 3D spruce model was conducted and tested at three structural levels, at the scale of shoot, tree crown, and canopy. Achieved results showed that use of the optimized 3D spruce model with a simplified shoot model (labeled as simple 1) and transformed into turbid cell mock-up yielded significantly better results when compared to outputs obtained with the traditional simpler spruce model. Besides higher accuracy estimates of canopy chlorophyll content and leaf area index retrieved from spectral remote sensing data through DART LUT inversion, this work contributed to new improvements of the DART model itself. Triggered by needs of this study, DART developers improved functions translating geometrical objects in turbid cell representations, introduced better model file management and optimized the DART code in general.

4.2 Potential improvements

One possible improvement of the 3D spruce model is creation of more realistic reference needle shoot model. The one used in this study was relatively simple, because it was designed for older versions of the DART model with limited capabilities of 3D objects handling. Moreover, it does not resemble the real natural distribution of individual needles along the central wooden twig. The architecture of each shoot varies depending on illuminations conditions, age and stress impacts. Precise 3D representation of shoot can be obtained from laboratory laser scanning. Although several shoot types were recreated this way, it was unfeasible to use them all within the framework of this thesis. The scanned shoots contain gaps, irregularities, and extremely high number of facets, which would require time demanding preprocessing. However, with a constant improvement of the DART model computational resources, we can expect its ability to process trees with more complex shoot models soon.

Similarly, it might be in future feasible to simulate larger forest scenes entirely reconstructed from airborne laser scanning data with the site-specific tree spatial and height distributions. Radiative transfer simulations of such scenes could facilitate retrievals of vegetation biochemical parameters from RS data fully customized to the study site conditions.

Additionally, a possible future extension of the algorithms creating the 3D models of trees is its adaptation to other coniferous or even further to broadleaf tree species.

4.3 Possible application of the 3D spruce model

In general, the 3D spruce model designed in this study can be used to understand better light interactions within a single tree crowns or whole canopies.

From RS perspective, one of the key issues in coniferous forest canopies is the upscaling of optical properties from needles, to shoots and to canopies. From operational point of view, it is easier to measure optical properties of needles rather than shoots. However, since shoots are the main scattering elements in the coniferous forest canopies, there is a strong demand to know shoot optical properties and phase functions with a high accuracy (Stenberg

1996, Smolander & Stenberg 2003, Rautiainen et al. 2012, and Mõttus et al. 2012). Traditional forest reflectance models, based on the radiative transfer equations, handle shoot level clumping by correcting the radiation attenuation coefficient with a clumping index, which simulates a reduction in the interception of radiation by the canopy at fixed LAI (Smolander & Stenberg 2003). Implementation of the precise 3D spruce model could help to disentangle and understand better light interaction related to the foliage clumping.

Finally, the 3D spruce model has been used to investigate scattering, reabsorption and angular isotropy of the chlorophyll fluorescence emissions produced by the plant cellular photosystems I and II. Results, presented at the Remote Sensing of Fluorescence, Photosynthesis and Vegetation Status Workshop (Malenovský et al. 2017), demonstrated a strong angular anisotropy of the top-of-canopy chlorophyll fluorescence signal caused by size, spatial geometry and clumping of spruce needles and shoots. Such sensitivity analyses contribute to full comprehension of this new vegetation optical signal, which will from 2022 be acquired by a new ESA satellite mission called FLEX (Drusch et al. 2016).

References

- Allen, W. A., Gausman, H. W., Richardson, A. J., & Thomas, J. R. (1969). Interaction of Isotropic Light with a Compact Plant Leaf. *Journal of the Optical Society of America*, 59(10), 1376–1379.
- Barták, M. (1992). *Struktura koruny smrku ztepilého ve vztahu k produkci* (Doctoral thesis). Institute of Systematic and Ecological Biology, Brno, Czech Republic
- Borovička, V., & Pazdera, J. (2009). *Technická zpráva - Zaměření dospělého smrkového porostu v lokalitě Černá hora - Šumava*. GEOVAP, spol.s r.o., Pardubice.
- CESBIO (2015) Centre d'Etudes Spatiales de la BIOSphère. DART Handbook (October 9, 2015)
- Chang, C.-C., & Lin, C.-J. (2011). LIBSVM: a library for support vector machines. *ACM Transactions on Intelligent Systems and Technology (TIST)*, 2(3), 27.
- Ciganda, V., Gitelson, A., & Schepers, J. (2009). Non-destructive determination of maize leaf and canopy chlorophyll content. *Journal of Plant Physiology*, 166(2), 157–167.
- Curran, P.J., Dungan, J.L., & Peterson, D.L. (2001). Estimating the foliar biochemical concentration of leaves with reflectance spectrometry: Testing the Kokaly and Clark methodologies. *Remote Sensing of Environment* 76, 349–359.
- Drusch, M., Moreno, J., Bello, U. D., Franco, R., Goulas, Y., Huth, A., ... Verhoef, W. (2016). The FLuorescence EXplorer Mission Concept-ESA's Earth Explorer 8. *IEEE Transactions on Geoscience and Remote Sensing*, PP(99), 1–12.
- Feret, J.-B., François, C., Asner, G.P., Gitelson, A.A., Martin, R.E., Bidel, L.P.R., Ustin, S.L., le Maire, G., & Jacquemoud, S. (2008). PROSPECT-4 and 5: Advances in the leaf optical properties model separating photosynthetic pigments. *Remote Sensing of Environment* 112, 3030–3043.
- Gastellu-Etchegorry, J.-P., Yin, T., Lauret, N., Cajgfinger, T., Gregoire, T., Grau, E., Feret, J.-B., Lopes, M., Guilleux, J., Dedieu, G. a kol (2015). Discrete Anisotropic Radiative Transfer (DART 5) for Modeling Airborne and Satellite Spectroradiometer and LIDAR Acquisitions of Natural and Urban Landscapes. *Remote Sensing* 7, 1667–1701.
- Gitelson, A.A., Gritz, Y., & Merzlyak, M.N. (2003). Relationships between leaf chlorophyll content and spectral reflectance and algorithms for non-destructive chlorophyll assessment in higher plant leaves. *Journal of Plant Physiology* 160, 271–282.
- Homolová, L., Lukeš, P., Malenovský, Z., Lhotáková, Z., Kaplan, V., & Hanuš, J. (2013). Measurement methods and variability assessment of the Norway spruce total leaf area: implications for remote sensing. *Trees*, 27(1), 111–121.
- Homolová, L., Malenovský, Z., Janoutová, R., Landier, L., Gastellu-Etchegorry, J.-P. (2015a). Technical note - Validation Database Description. Red Edge Positioning (REP) Techniques for Earth Observation Optical Missions (AO/1-7600/13/NL/LvH). Published by European Space Agency (p.38)

- Homolová, L., Malenovský, Z., Janoutová, R., Landier, L., Crochet, T., Berthelot, B. (2015b). Algorithm Theoretical Basis Document - Retrieval of Biophysical Variables: Leaf Chlorophyll Content and Leaf Area Index (REDEDGE-CG-CESBIO-ATBD-03-0002). Red Edge Positioning (REP) Techniques for Earth Observation Optical Missions (AO/1-7600/13/NL/LvH). Published by European Space Agency (p.88).
- Jacquemoud, S., & Baret, F. (1990). PROSPECT: a model of leaf optical properties spectra. *Remote Sensing of Environment* 34, 75–91.
- Jacquemoud, S., Verhoef, W., Baret, F., Bacour, C., Zarco-Tejada, P.J., Asner, G.P., François, C., and Ustin, S.L. (2009). PROSPECT + SAIL models: a review of use for vegetation characterization. *Remote Sensing of Environment* 113, Supplement 1, S56–S66.
- Janoutová, R. (2012). Mathematical methods of morphology modelling of coniferous trees. Brno University of Technology. Brno: Vysoké učení technické v Brně, Fakulta strojního inženýrství, pp. 51.
- Jones, H. G. & Vaughan, R. A. (2010). *Remote sensing of vegetation: principles, techniques, and applications*. Oxford University Press, Oxford ; New York
- Liang, S. (2005). *Quantitative Remote Sensing of Land Surfaces* (John Wiley & Sons).
- Main, R., Cho, M.A., Mathieu, R., O’Kennedy, M.M., Ramoelo, A., & Koch, S. (2011). An investigation into robust spectral indices for leaf chlorophyll estimation. *ISPRS Journal of Photogrammetry and Remote Sensing* 66, 751–761.
- Malenovský, Z., Albrechtová, J., Lhotáková, Z., Zurita-Milla, R., Clevers, J. G. P. W., Schaepman, M. E., & Cudlín, P. (2006). Applicability of the PROSPECT model for Norway spruce needles. *International Journal of Remote Sensing*, 27(24), 5315–5340.
- Malenovský, Z., Gastellu-Etchegorry, J.-P., Lauret, N., Yin, T., Guilleux, J., Chavanon, E., Janoutová, R., Verhoef, W., van der Tol, C., Cook, B., Morton, D., & Middleton, E.M. (2017). Discrete Anisotropic Radiative Transfer (DART) modelling of chlorophyll fluorescence in three-dimensional structurally explicit plant canopies [poster]. In *Remote Sensing of Fluorescence, Photosynthesis and Vegetation Status Workshop*.
- Möttus, M., Rautiainen, M., & Schaepman, M. E. (2012). Shoot scattering phase function for Scots pine and its effect on canopy reflectance. *Agricultural and Forest Meteorology*, 154–155, 67–74.
- Rautiainen, M., Möttus, M., Yáñez-Rausell, L., Homolová, L., Malenovský, Z., & Schaepman, M. E. (2012). A note on upscaling coniferous needle spectra to shoot spectral albedo. *Remote Sensing of Environment*, 117, 469–474.
- Schlerf, M., & Atzberger, C. (2006). Inversion of a forest reflectance model to estimate structural canopy variables from hyperspectral remote sensing data. *Remote Sensing of Environment* 100, 281–294.
- Sloup, P. (2013). *Automatic Tree Reconstruction from its Laser Scan*. Master Thesis. Masaryk University Faculty of Informatics, Brno, (p.74).
- Sloup, P., Rebok, T. & Hanuš, J. (2013). *Automatic Tree Reconstruction from its Laser Scan* [poster]. In *Global Change and Resilience*, Brno.

- Smola, A. J., & Schölkopf, B. (2004). A tutorial on support vector regression. *Statistics and Computing*, 14(3), 199–222.
- Smolander, S., & Stenberg, P. (2003). A method to account for shoot scale clumping in coniferous canopy reflectance models. *Remote Sensing of Environment*, 88(4), 363–373.
- Stenberg, P. (1996). Simulations of the effects of shoot structure and orientation on vertical gradients in intercepted light by conifer canopies. *Tree Physiology*, 16(1), 99–108.
- Stuckens, J., Dzikiti, S., Verstraeten, W. W., Verreyne, S., Swennen, R., & Coppin, P. (2011). Physiological interpretation of a hyperspectral time series in a citrus orchard. *Agricultural and Forest Meteorology*, 151(7), 1002–1015.
- Verrelst, J., Alonso, L., Camps-Valls, G., Delegido, J., & Moreno, J. (2012a). Retrieval of Vegetation Biophysical Parameters Using Gaussian Process Techniques. *IEEE Transactions on Geoscience and Remote Sensing* 50, 1832–1843.
- Verrelst J, Muñoz J, Alonso L, et al. (2012b). Machine learning regression algorithms for biophysical parameter retrieval: Opportunities for Sentinel-2 and -3. *Remote Sensing of Environment* 118, 127–139.

Curriculum vitae

Ing. Růžena Janoutová

e-mail janoutova.r@gmail.com

EDUCATION

Doctoral studies 2012 - 2017	Brno University of Technology Faculty of Mechanical Engineering Applied Mathematics Dissertation: <i>Modelling 3D forest structure for improved retrieval of forest biophysical properties.</i> Supervisor: doc. PaedDr. Dalibor Martišek, Ph.D.
Master's degree 2010 - 2012	Brno University of Technology Faculty of Mechanical Engineering Mathematical Engineering
Bachelor's degree 2007 - 2010	Brno University of Technology Faculty of Mechanical Engineering Mathematical Engineering

WORK EXPERIENCE

2014 - 2015	Centre d'Etudes Spatiales de la BIOSphère in France Internship
2012 - now	Global Change Research Institute CAS Radiative transfer modelling.

Abstract

The main goal of the thesis was to improve quantitative estimation of vegetation parameters of spruce stand using spectral simulations of three-dimensional radiative transfer model. In the first step, the precise computer 3D model of a spruce tree was created. Since implementation of such precise representation was for a larger forest canopy computationally too demanding, the 3D model had to be simplified. The optimal simplification was found using available spectral airborne data and through comparison with the original 3D spruce model. The optimal simplification yielded an acceptable compromise between computation requirements and accuracy of radiative transfer simulations reproducing the forest stand reflectance. The optimized simplification was subsequently used in retrievals estimating the vegetation parameters from a spectral satellite image. Accuracy of the estimates was validated through comparison with field measurements of retrieved parameters.

Finally, the results obtained after implementation of new optimal 3D spruce model were compared with results obtained using a more traditional approach based on geometrically simpler tree crown shapes.

Abstrakt

Hlavním cílem práce bylo zlepšení kvantitativních odhadů vegetačních parametrů smrkových porostů pomocí spektrálních simulací trojrozměrného modelu přenosu záření. Prvně bylo potřeba vytvořit přesný 3D model smrku. Implementace přesného 3D modelu smrku pro parametrizaci celých lesních porostů je v současné době výpočetně nemožné, bylo tedy nutné tento 3D model smrku zjednodušit. Přesný 3D model smrku společně s dostupnými leteckými daty sloužil pro nalezení optimálního zjednodušení. Optimální model vedl ke kompromisu mezi výpočetní náročností a přesností výsledné odrazivosti z modelu přenosu záření. Následně byl optimální model smrku využit pro odhady vegetačních parametrů ze satelitních snímků. Přesnost odhadů byla ověřena oproti pozemním měřením odhadovaných parametrů. Na závěr byly porovnány výsledky z odhadů vegetačních parametrů pomocí optimálního 3D modelu smrku s výsledky z tradičního přístupu pomocí modelů stromu s geometricky jednoduššími tvary korun.